AD A044560

BRL R 2007

BRL

AD

12

B.S.

REPORT NO. 2007

APPLICATION OF LASER PROBING TO BALLISTIC METEOROLOGY

Jad H. Batteh

August 1977

Approved for public release; distribution unlimited.

DDC
RECEIVED
SEP 27 1977
B

DDC FILE COPY

USA ARMAMENT RESEARCH AND DEVELOPMENT COMMAND
USA BALLISTIC RESEARCH LABORATORY
ABERDEEN PROVING GROUND, MARYLAND

Destroy this report when it is no longer needed.
Do not return it to the originator.

Secondary distribution of this report by originating or sponsoring activity is prohibited.

Additional copies of this report may be obtained from the National Technical Information Service, U.S. Department of Commerce, Springfield, Virginia 22151.

The findings in this report are not to be construed as an official Department of the Army position, unless so designated by other authorized documents.

The use of trade names or manufacturers' names in this report does not constitute indorsement of any commercial product.

UNCLASSIFIED

SECURITY CLASSIFICATION OF THIS PAGE *(When Data Entered)*

REPORT DOCUMENTATION PAGE		READ INSTRUCTIONS BEFORE COMPLETING FORM
1. REPORT NUMBER BRL Report No. 2007	2. GOVT ACCESSION NO.	3. RECIPIENT'S CATALOG NUMBER
4. TITLE *(and Subtitle)* Application of Laser Probing to Ballistic Meteorology.		5. TYPE OF REPORT & PERIOD COVERED 6. PERFORMING ORG. REPORT NUMBER
7. AUTHOR(s) Jad H. Batteh		8. CONTRACT OR GRANT NUMBER(s)
9. PERFORMING ORGANIZATION NAME AND ADDRESS Ballistic Research Laboratory Aberdeen Proving Ground, MD 21005		10. PROGRAM ELEMENT, PROJECT, TASK AREA & WORK UNIT NUMBERS 1T161101A91A
11. CONTROLLING OFFICE NAME AND ADDRESS US Army Materiel Development and Readiness Command 5001 Eisenhower Avenue Alexandria, VA 22333		12. REPORT DATE AUGUST 1977 13. NUMBER OF PAGES 36
14. MONITORING AGENCY NAME & ADDRESS*(if different from Controlling Office)*		15. SECURITY CLASS. *(of this report)* Unclassified 15a. DECLASSIFICATION/DOWNGRADING SCHEDULE

16. DISTRIBUTION STATEMENT *(of this Report)*

Approved for public release; distribution unlimited.

DDC
RECEIVED
SEP 27 1977
B

17. DISTRIBUTION STATEMENT *(of the abstract entered in Block 20, if different from Report)*

18. SUPPLEMENTARY NOTES

19. KEY WORDS *(Continue on reverse side if necessary and identify by block number)*

Laser Probing, Lidar, Ballistic Meteorology

20. ABSTRACT *(Continue on reverse side if necessary and identify by block number)*

(hmn)

Laser probing of the atmosphere is reviewed with particular emphasis on its application to ballistic meteorology. The requirements of the meteorological system are discussed, and the shortcomings of the rawinsonde technique, currently used, are outlined. A brief description of the relevant interactions of laser radiation with the atmosphere is presented. The potential of laser probing techniques for atmospheric measurements, as well as their current limitations, are then discussed in some detail. It is concluded that a system based on

DD FORM 1 JAN 73 1473 EDITION OF 1 NOV 6 IS OBSOLETE

UNCLASSIFIED

SECURITY CLASSIFICATION OF THIS PAGE *(When Data Entered)*

Aremote sensing with lasers is capable of timely and accurate measurements of all the relevant meteorological variables. However, present systems are unable to attain the maximum range required for ballistic applications.

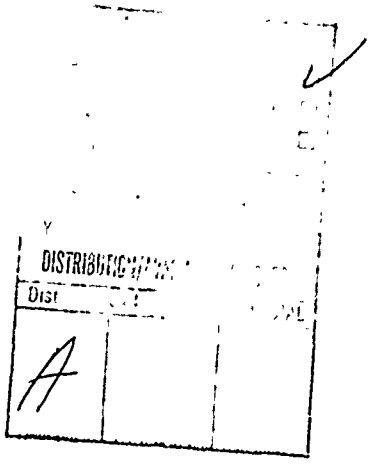

TABLE OF CONTENTS

I. INTRODUCTION

The trajectory of an artillery shell depends not only on its initial momentum and the force of gravity, but also on the viscous and buffeting forces it encounters during its flight. The artillery unit can partially compensate for these atmospheric forces by referring to the firing tables which give corrections to the aim based on detailed trajectory calculations for a variety of atmospheric conditions. To make proper use of the firing tables, the atmosphere near the artillery site must be probed before firing, and this responsibility lies with the meteorology team assigned to the artillery unit.

The relevant meteorological variables are the air density and temperature, the humidity and the wind velocity. Currently, these variables are determined by an instrumented balloon which probes the atmosphere as it ascends and radios the information to a ground receiving station. The time required to complete a sounding, usually two to four hours, is determined primarily by the slow rise rate of the balloon. Since the atmospheric conditions may undergo marked changes on this time scale, the meteorological variables measured by the balloon may no longer be representative of the conditions actually encountered by the projectile along its trajectory.

Clearly, the time delay in the present system limits the usefulness of the firing tables, and alternative techniques for sounding the atmosphere should be explored. Ideally, the measurements should be made remotely, thereby eliminating the need for a sensor to traverse the atmosphere. At present, there is no system which can be deployed on the battlefield that is capable of remotely measuring the density, temperature, humidity and wind velocity to the required altitude, roughly 20 km. However, atmospheric sounding with high power lasers, commonly referred to as lidar (light detection and ranging), appears to be a promising candidate for the future. With lidar, the meteorological variables are determined from the backscattered radiation which results when a laser beam interacts with the atmosphere; therefore, the need for artificial sensors is eliminated. First applied to the study of scattering in the mesosphere, lidar has since been used to measure a wide variety of atmospheric parameters, including density, temperature, humidity and wind velocity. Since the sounding is accomplished by radiation which travels at the speed of light, a lidar system is potentially capable of providing prompt meteorological data to the artillery unit. In fact, the system could be operated continuously so that any changes in the atmospheric conditions during a long engagement could be relayed to the artillery team. Lidar has the additional advantage that sampling in different directions can be achieved by simply rotating the transmission optics and the receiving antenna, whereas in the present system the probed volume is fixed by the balloon trajectory.

As mentioned previously, no system based on remote probing, including lidar, is currently capable of satisfying the requirements of ballistic meteorology. However, advances in laser technology and detection techniques, which will result from research in this as well as unrelated areas, will undoubtedly narrow the gap between the capability of lidar probes and the needs of a ballistic system. The importance of lidar to ballistics lies in this promise and in the proven feasibility of laser probing to measure all the relevant meteorological variables.

This report reviews the status of laser probing of the atmosphere as it relates to ballistic meteorology. It begins with a discussion of the probing technique currently used by the Army and its limitations. Then, a brief review of the interaction of laser beams with the atmosphere sets the foundation for the remainder of the report, which details the current status of lidar techniques for measuring density, humidity, temperature and wind velocity.

II. THE BALLISTIC METEOROLOGICAL MESSAGE

The meteorological data gathered from atmospheric soundings is reduced by the meteorology team and transmitted to the artillery in the form of a ballistic message. The message consists of the calculated values of the ballistic wind, ballistic density and ballistic temperature at selected heights. The ballistic wind is a wind of constant speed and direction which would have the same total effect on the projectile during its flight as the varying winds actually encountered. The ballistic density and temperature are defined in a similar manner.

For calculation of the ballistic quantities, the atmosphere from the surface to 20 km is divided into a number of horizontal zones. The height of each zone varies from .2 km to 2 km depending on the particular zone[1]. Average values for the horizontal wind, density and virtual temperature are deduced from the sounding for each zone. (The virtual temperature is the temperature of dry air at the same pressure which has a density equivalent to that of the moist air encountered.) The deviations of these averages from established standard values are then calculated for each zone. A weighted average of the differences is used to calculate the ballistic quantities for each zone. The empirically determined weighting factors reflect the importance of the properties in each zone on the overall trajectory of the projectile. For example, since a surface to surface artillery shell spends most of its time

1. Department of the Army Field Manual FM 6-15, Artillery Meteorology (1970).

near the top of its trajectory, the weighting factor is greatest for the zone which includes the trajectory apex. The artillery unit uses the ballistic parameters for the zone which contains the maximum ordinate of the shell trajectory to determine from the firing tables the corrections to the gun elevation and azimuth. Alternatively, the meteorological data may be fed into the Field Artillery Digital Automatic Computer (FADAC) which provides the corrections after actually solving for the ballistic trajectory.

III. THE RAWINSONDE SYSTEM AND ITS LIMITATIONS

Artillery meteorological data is currently obtained from a rawinsonde system[1], consisting of a radiosonde, a rawin set and a radiosonde recorder. The radiosonde is a balloon-borne, battery-powered sensor which automatically measures pressure, temperature and humidity, and transmits this information to a ground receiving station via radio waves. The receiver, a rawin set, is a radio direction finder which tracks the radiosonde throughout its flight, measuring the elevation and azimuth angles to the radiosonde. The rawin set also receives and demodulates the transmitted weather signal, which is then sent to the recorder. The rawinsonde system provides all-weather capability for atmospheric sounding to an altitude of 30 km.

The vertical profiles of temperature, density, humidity and horizontal wind velocity are the atmospheric parameters required to calculate the ballistic meteorological message. The temperature, pressure and humidity profiles are measured directly by the radiosonde and the density is determined from the perfect gas law,

$$p = \rho RT \tag{3.1}$$

where p is the pressure, ρ is the density, R is the gas constant for air and T is the temperature.

Since balloons are faithful wind tracers, the radiosonde trajectory provides a measurement of the horizontal wind. Calculation of the trajectory requires knowledge of the balloon height, elevation angle and azimuth angle as functions of time. The elevation and azimuth angles are measured directly by the rawin set as it tracks the radiosonde. The height can be approximated from the hydrostatic equation which relates the variation of pressure with altitude, Z, to the density[2]

2. U.S. Standard Atmosphere, 1962 (US Government Printing Office, Washington, 1962) Ch. 1.

$$\frac{dp}{dZ} = - \rho g \tag{3.2}$$

where g is the acceleration due to gravity. Using the perfect gas law, we can write Eq. (3.2) as

$$Z_2 - Z_1 = - \frac{R}{g} \int_{p_1}^{p_2} \left(\frac{T}{p}\right) dp \tag{3.3}$$

where Z_2 and Z_1 are the altitudes corresponding to the pressure readings p_2 and p_1, respectively. Therefore, the difference in elevation between two readings can be approximated by

$$Z_2 - Z_1 = - \frac{R\bar{T}}{g} \ln\left(\frac{p_2}{p_1}\right) \tag{3.4}$$

where $\bar{T}$ is the average temperature over the interval.

In case of equipment failure, a back-up system is employed. In this case, the departure method is used to estimate the temperatures and densities from values measured at the surface[1]. The temperature is assumed to vary with height according to the standard ICAO atmospheric lapse rate. The calculation of density is based on research in climatology which indicates a correlation between the density at the surface and the densities aloft. The principle is used to provide climatological tables which contain values of upper air densities corresponding to specific regions of the world, time of day and measured surface conditions. Ballistic winds are estimated by tracking an uninstrumented balloon (pilot balloon) with a theodolite to measure the azimuth and elevation angles. An assumed rate of rise is used to provide altitude information. Obviously, the ballistic quantities derived from the departure-pilot balloon method are far less reliable than the values obtained from the rawinsonde system.

The time required to complete a sounding with the rawinsonde system is determined primarily by the slow ascent rate of the balloon and usually varies from two to four hours depending on the maximum altitude to be probed. Also, the balloon can only measure conditions along its path, which may be tens of kilometers distant from the mid-point of the shell trajectory. These problems of time staleness and space separation raise the question of whether the properties measured by the radiosonde are representative of the conditions the projectile will actually encounter during its flight. The answer to this question, of course, depends on the geographic location and the prevailing weather conditions.

For example, large spatial variations in wind velocity are associated with mountainous terrain, an effect which extends to heights much greater than the mountain tops, and space scales of a kilometer and time scales of an hour are typical for certain mesoscale phenomena such as thunderstorms, fronts and sea breezes[3].

The effect of space separation and time staleness on firing accuracy has been the subject of several investigations[4-7]. In one test[4,5] conducted at Fort Sill, Okalahoma, 105mm and 8 in. howitzers were fired at targets located at a distance of 9 km. The azimuth and elevation angles of the howitzers were obtained from the firing tables based on meteorological data with a staleness of 0 to 6 hours. The effect of space separation was investigated by varying the distance between the sounding location and the artillery unit from 1.6 to 80 km. The study concluded that

1. A distance of 30 km between the meteorology station and the artillery unit was not significant.

2. At 80 km, the error due to separation increased by a factor of two or three over the error at 30 km, depending on the direction of the meteorology station from the artillery unit.

3. Errors due to staleness are more important. For time delays of two to six hours, the meteorological error is appreciably greater than the ballistic error of the weapon.

These and other tests have shown that the aiming error increases as a function of the square root of both the time delay and the separation[5,6]. Although it should be emphasized that the results are highly dependent on the experimental conditions, it can be concluded that time staleness and, to a lesser extent, space separation severely limit the usefulness of present sounding methods.

---

3. E.R. Reiter, "Fundamental Problems of Atmospheric Science", in Remote Sensing of the Troposphere, edited by V.E. Derr (US Government Printing Office, Washington, 1972).
4. O.P. Bruno, "Effects of Ballistic and Meteorological Variables On Accuracy of Artillery Fire", BRL Memorandum Report 1210, US Army Ballistic Research Laboratories, 1959. (AD #219226)
5. R. Bellucci, "Analysis of Ballistic Meteorological Effects on Artillery Fire", USASRDL Technical Report 2224, 1961.
6. K.M. Barnett, E.A. Blomerth and H.H. Monahan, "Plan for the Atmospheric Sciences Laboratory Artillery Meteorological Comparisons", US Army ECOM, 1974.
7. J.H. Shinn and H.W. Maynard, "On the Sensitivity of Selected Typical Army Operations to Weather Effects", US Army ECOM-5547, 1974.

A significant reduction in the sounding time can be achieved by remote probing of the atmosphere since remote probing eliminates the need for introducing instrumentation into the region to be sampled. Remote sensing of the atmosphere also has the capability of continuously monitoring the atmosphere so that temporal changes can be easily detected. None of the three types of remote sensing techniques, optical, radio or acoustic, can currently measure all the necessary meteorological parameters at the ranges of ballistic interest and with the resolution required. But of the three, optical sensing with high-power lasers appears to have the greatest potential for satisfying the needs of a ballistic system. In the following sections, we will discuss laser probing of the atmosphere with particular emphasis on its potential application to ballistic meteorology.

IV. INTERACTION OF LASER RADIATION WITH THE ATMOSPHERE

Laser radiation propagating in the atmosphere is subject to a number of interactions, including absorption, scattering, line broadening and frequency shift. These interactions can be exploited to remotely determine atmospheric parameters. Atmospheric probing with lasers, commonly referred to as lidar, was first applied in 1963 by Fiocco and Smullin[8] to the study of scattering in the mesosphere and since then has become an important tool in atmospheric research and meteorological observation. The interested reader may find the review articles, Refs. 9-12, as well as the bibliography compiled by Harris[13] useful guides to this rapidly expanding field. In this section, we will describe the operation of a basic lidar system and then review the absorption and scattering properties of the atmosphere as they pertain to laser probing.

---

8. G. Fiocco and L.D. Smullin, "Detection of Scattering Layers in the Upper Atmosphere (60-140 km) by Optical Radar", Nature 199, 1275, (1963).
9. O.K. Kostko, "Use of Laser Radar in Atmospheric Investigations (Review)", Sov. J. Quant. Electron. 5, 1161 (1976).
10. C.P. Wang, "Application of Lasers in Atmospheric Probing", Acta Astron. 1, 105 (1974).
11. R.T.H. Collis, "LIDAR", Appl. Opt. 9, 1782 (1970).
12. R.G. Strauch and A. Cohen, "Atmospheric Remote Sensing With Laser Radar", in Remote Sensing of the Troposphere edited by V.E. Derr (US Government Printing Office, Washington, 1972).
13. F.S. Harris, "Laser Applications to Atmospheric Sciences - A Bibliography", NASA CR-2536, 1975.

In general, the lidar system consists of a laser and its associated transmission optics, a receiver to collect the scattered radiation, and the electro-optics required to process the return signal. Frequency filters are often used in the receiver so that a specific interaction may be probed. In battlefield applications the separation between the transmitter and receiver will be much smaller than the range to the probed volume so that the radiation detected will be the radiation scattered at an angle of 180° to the direction of the incident beam.

For short ranges, a focused continuous laser can be used with the range selectivity provided by varying the focal length of the transmission optics. However, as the focal length is increased the length of the region enclosed by the half-power points of the beam also increases. This increase in the length of the scattering volume results in a decrease in the resolving capability of the lidar according to[14]

$$\Delta R = \frac{2\lambda R^2}{A_t} \tag{4.1}$$

where ΔR is the range resolution, R is the range to the probed volume, A_t is the area of the transmitter lens and λ is the wavelength of the laser radiation. Consequently, the focused lidar system is only useful for measurements at low altitudes (typically less than a kilometer).

For ranges beyond a kilometer, a system based on an unfocused, pulsed laser source must be used to provide adequate range resolution. Since the laser pulse illuminates a well-defined volume at any given time, the volume to be probed is selected by time-gating the receiver. The range resolution for a pulsed system is determined by the volume of the atmosphere which contributes to the signal during the time t_r the receiver is opened. For a laser pulse of temporal length t_p,

$$\Delta R \simeq \tfrac{1}{2}\, c\, (t_p + t_r) \tag{4.2}$$

where c is the speed of light. In this case, the resolution is independent of range in contrast to the R^2 variation characteristic of the focused system. Therefore, lidar applications to ballistic meteorology will require a system based on a pulsed laser and time-gated receiver in order to achieve adequate spatial resolution at altitudes of several kilometers.

The intensity of the received signal per transmitted pulse from the probed volume at range R is given by the laser radar equation[12]

14. T.R. Lawrence, D.J. Wilson, C.E. Craven, L.P. Jones, R.M. Huffaker and J.A.L. Thomson, "A Laser Velocimeter for Remote Wind Sensing", Rev. Sci. Inst. 43, 512 (1972).

$$N_r(R,\lambda_s,\lambda) = \frac{N_t \rho_s(\lambda_s,\lambda,R)\sigma_s(\lambda_s,\lambda)\eta\, A_r \Delta R}{R^2}$$

$$\times \exp\left\{ -\int_o^R \left[\beta(\lambda) + \beta(\lambda_s)\right] dr \right\} \tag{4.3}$$

where

λ = transmitted laser wavelength

λ_s = wavelength of the scattered signal which is detected

N_t = number of photons transmitted per pulse

N_r = number of photons of wavelength λ_s received from range R per transmitted pulse

ρ_s = number density of scatterers at range R which scatter the incident radiation into radiation of wavelength λ_s

σ_s = backscatter cross-section for the interaction in m^2/ster.

$\beta(\lambda)$ = extinction coefficient at the wavelength λ in m^{-1}.

η = lumped efficiency factor for the transmitting, collimating, receiving and detecting systems.

A_r = area of the receiver.

ΔR = length of the probed volume in the direction of the transmitted signal as given by Eq. (4.2).

The exponential term accounts for the decrease in intensity of the transmitted pulse in propagating to the probed volume, and the decrease in intensity of the scattered radiation as it propagates back to the detector. The extinction coefficient, which includes molecular and aerosol scattering and molecular absorption, depends on the frequency of the radiation, the density and the aerosol content along the laser path.

The laser radar equation is generally used to deduce the vertical profile of the number density of scatterers, ρ_s, from the intensity of the received signal, N_r, at various altitudes. The inversion is complicated by the fact that the extinction coefficients will not be known a priori since they depend on the density and aerosol content. Furthermore, the Mie scattering coefficient for aerosols is difficult to calculate theoretically since it depends on the size, shape and

composition of the aerosol. Finally, the efficiency factor must usually be determined experimentally. Actually, Eq. (4.3) can be simplified somewhat since absorption can be neglected unless the wavelength corresponds to a molecular absorption line. Also, for wavelengths which do not correspond to resonant scattering events, the scattering cross sections are sufficiently low that the extinction term can be neglected altogether for probing at altitudes less than a few kilometers, provided that the aerosol concentration is not too high. And in one instance, namely the lidar detection of wind velocity, the measurement can be made without the need of inverting the laser radar equation.

In the remainder of this section, we will briefly review the relevant scattering and absorption processes which occur when a laser beam propagates through the atmosphere; this will set the foundation for the remaining sections which will discuss the state of the art of lidar measurements of density, wind velocity, humidity and temperature.

1. Rayleigh Scattering.

Rayleigh scattering is an elastic interaction which occurs in a gas when the incident frequency of the radiation is far from any absorption line of the gas molecul The frequency spectrum of the Rayleigh backscatter will be bell-shaped with the maximum intensity occurring at the frequency of the incident radiation. The broadening of the frequency spectrum is due to the Doppler shift resulting from the thermal motion of the molecules.

The backscatter cross section per molecule for Rayleigh scattering is given by[12]

$$\sigma_R = \frac{\pi^2 (n-1)^2}{\rho_s^2 \lambda^4} \quad \frac{6+3\delta}{6-7\delta} \tag{4.4}$$

where ρ_s is the molecular number density, n is the index of refraction for a standard atmosphere and δ is a depolarization factor approximately equal to .035 for air molecules. For infrared laser radiation, the Rayleigh cross section in air is typically on the order of $10^{-31} m^2/ster$.

If the dominant interaction at the laser frequency is Rayleigh scattering, then $\lambda_s \approx \lambda$, $\sigma_s = \sigma_R(\rho_s)$ and $\beta = \rho_s \sigma_R(\rho_s)$. In that case, the laser radar equation, Eq. (4.3), is a function only of ρ_s so that the return signal provides a measurement of the density of scatterers as a function of range. At high altitudes, the Rayleigh scattering can be used directly as outlined above to measure density; however, in the lower atmosphere the interpretation of the return signal is

complicated since the elastic backscatter will have an additional component due to scattering from aerosols.

2. Mie Scattering.

Another important interaction in the lower atmosphere is Mie scattering of the incident radiation off suspended aerosols. Although the size, composition and number density of aerosols varies with location and weather conditions, they are always present to some degree even under the clearest conditions. The number density of aerosols is small averaging only about $10^3/cm^3$ in the layer from the ground to 10 km, but the aerosol contribution to the total backscatter is significant since the cross section per particle can be quite large. It is difficult to accurately calculate the Mie cross section for atmospheric aerosols since it depends strongly on the size, shape and composition of the particles, but the cross section generally varies between 10^{-31} and $10^{-12} m^2/ster$. The aerosols in the atmosphere are not stationary but are swept along by the mean wind. (In fact, their small inertia and fast response time makes them excellent tracers for measuring the wind velocity. This point is discussed in greater detail in the Appendix.) Consequently, the Mie scattered radiation will exhibit a Doppler shift in frequency characteristic of the local wind velocity. The Mie contribution to the total backscatter will appear as a narrow spike embedded in the much broader Rayleigh spectrum.

3. Raman Scattering.

In addition to the elastic Rayleigh interaction, molecules can scatter energy inelastically through Raman scattering. In a Raman interaction, the frequency of the scattered radiation is changed by an amount characteristic of the energy difference between two vibrational-rotational states of the molecule. Since the frequency shift of the scattered radiation allows identification of the individual scatterer, Raman scattering with laser sources is a powerful tool for measuring density, temperature and species concentration. The Raman scattering cross section is proportional to[10]

$$\sigma_{Raman} \sim \frac{(\nu_i-\nu)^4 (45\alpha^2+7\gamma^2)}{1-\exp(-h\nu/kT)} \qquad (4.5)$$

where ν_i and ν are the frequencies of the incident and scattered radiation, respectively, α is the isotropic part of the polarizability change, γ is the anisotropic part of the polarizability change and T is the gas temperature. Unfortunately, Raman scattering is a weak interaction; typically, cross sections for atmospheric gases are on

the order of 10^{-33} to 10^{-34} m^2/ster. However, if a laser frequency is chosen which is near the frequency of an allowed transition, there is a resonance effect which enhances the cross section approximately as[10]

$$\sigma'_{\text{Raman}} \sim \sigma_{\text{Raman}} \frac{4\nu_i^2}{4(\nu_i-\nu_T)^2 + (\Delta\nu)^2} \tag{4.6}$$

where ν_T is the frequency of the allowed transition and $\Delta\nu$ is its line width. This resonance effect can increase the cross section by several orders of magnitude over the nonresonant cross section.

4. Resonance Scattering (Fluorescence).

If the incident frequency coincides with an absorption line of the molecule, transition to the resonant state occurs followed by relaxation and emission of radiation. Since the absorption lines or bands are specific to the molecule, resonance scattering is another method for obtaining the number density of individual species. Due to the resonance effect, the cross sections are very high, on the order of 10^{-23} to 10^{-21} m^2/ster. However, there are several limitations on the use of resonance scattering in atmospheric measurements. First, the laser frequency must correspond to an allowed transition of the molecule to be probed. Furthermore, if the transition occurs to an excited state with a long fluorescence decay time, the range resolution of the system could be degraded. Also, quenching of the fluorescence becomes important if the fluorescence decay time is much greater than the collisional relaxation time of the excited molecule. Finally, radiation trapping of the fluorescence poses a severe problem. It not only reduces the intensity of the return, thereby limiting the range, but also delays the backscattered radiation, complicating the inversion of the laser radar equation.

5. Resonance Absorption.

In general, the absorption cross section at the center of an absorption line is several orders of magnitude larger than the cross section in the wings. It is possible to take advantage of this resonance effect to measure the number density of a species whose absorption frequency coincides with the emission frequency of a laser. In this technique, the laser is tuned to the center of the absorption line, and a measurement is made of the backscatter at the laser frequency as a function of range. A second measurement is then taken with the laser tuned to a relatively absorption free spectral region. The nonresonant absorption and scattering contributions to the return signal will be the same for both measurements if the two wavelengths

are close together. Consequently, the intensity of the received signal at the resonant wavelength can be written from Eq. (4.3) as

$$N'(R) = N(R) \exp\left[-2\int_o^R n(r)\,\sigma_{res}(r)dr\right] \tag{4.7}$$

where N' and N are the intensities of the received signal at the resonant and nonresonant wavelengths, respectively, n is the number density of resonant absorbers and σ_{res} is the resonant contribution to the absorption cross section. The density $n(R)$ can then be obtained from Eq. (4.7) in terms of the derivative of the ratio of the two returns,

$$n(R) = -\frac{1}{2\sigma_{res}(R)}\frac{d}{dR}\left[\ell n\left(\frac{N'}{N}\right)\right]. \tag{4.8}$$

There are two major difficulties associated with the resonant absorption technique. First, the laser frequency must coincide with the absorption line of the molecule to be probed in order to take advantage of the resonance. Secondly, the number density is derived from the gradient of the ratio of the two signals. Derivatives are essentially noisy so that an error in the ratio results in an amplified error in the number density.

With this background, we now proceed to a discussion of how these interactions can be exploited to determine the meteorological variables.

V. LIDAR MEASUREMENTS OF DENSITY AND HUMIDITY

As noted in Sec. IV, the density can be determined directly from the intensity of the backscattered signal if Rayleigh scattering is the dominant interaction. However, at the altitudes of interest to ballistic meteorology, the contribution of aerosols to the total elastic scattering is significant, and it is necessary to extract the component due to Rayleigh scattering from the total backscatter. Of course, one could assume an aerosol distribution and cross section and thereby estimate the Mie component of the backscatter, but this is clearly unsatisfactory since Mie scattering is strongly dependent on the shape, size and composition of the aerosol. One experimental technique for extracting the component due to Rayleigh scattering takes advantage of the different wavelength dependence of the two interactions. As indicated by Eq. (4.4) the cross section for Rayleigh scattering decreases dramatically with increasing wavelength ($\sigma_R \propto \lambda^{-4}$), whereas the cross section for Mie scattering exhibits a much weaker dependence on wavelength. Therefore, the relative contributions of the two processes can be determined by probing the same

volume with two laser beams of different frequencies. The feasibility of the two-wavelength technique was demonstrated by Zakharov and his associates[9]. They were able to determine the atmospheric density profile to a height of 15 km by comparing the backscatter from a pulsed ruby laser (λ = 694.3 nm) with the backscatter from a doubled Nd laser (λ = 530.0 nm).

Alternatively, the density can be measured by monitoring the Raman component of the backscatter due to nitrogen molecules. The Raman contribution can be easily separated from both the Rayleigh and Mie components since it is shifted in frequency by an amount characteristic of a specific vibration-rotation line of N_2. The major disadvantage of this method is the small cross section for Raman scattering, which results in extremely weak return signals unless powerful lasers are used. Even then the return must be integrated over tens of pulses to achieve a detectable signal. Nevertheless, Leonard[15] in 1967 and subsequently Cooney[16] and Melfi, et al.[17,18] were able to observe Raman scattering from nitrogen in the atmosphere. Since their experiments were limited to a maximum altitude of a few kilometers, the extinction of the transmitted and scattered signals could be neglected, and the nitrogen density could be determined directly from the intensity of the Raman backscatter. With a large lidar system, based on a pulsed ruby laser capable of 10 joules in 10 μsec, Garvey and Kent[19] were able to detect Raman scattering from nitrogen at altitudes between 15 and 40 km. In order to determine the density from the returns at these altitudes, however, it would be necessary to account for the extinction of the signals by monitoring the Rayleigh and Mie backscatter.

15. D. Leonard, "Observation of Raman Scattering from the Atmosphere Using a Pulsed Nitrogen Ultraviolet Laser", Nature 216, 142 (1967).
16. J.A. Cooney, "Measurements on the Raman Component of Laser Atmospheric Backscatter", Appl. Phys. Lett. 12, 40 (1968).
17. S.H. Melfi, J.D. Lawrence, and M.P. McCormick, "Observation of Raman Scattering by Water Vapor in the Atmosphere", Appl. Phys. Lett. 15, 295 (1969).
18. S.H. Melfi, "Remote Measurements of the Atmosphere Using Raman Scattering", Appl. Optics 11, 1605 (1972).
19. M.J. Garvey and G.S. Kent, "Raman Backscatter of Laser Radiation from the Stratosphere", Nature 248, 124 (1974).

Raman scattering has also been used to measure the density of water molecules in the atmosphere to a height of a few kilometers [17,18,20,21]. In fact, the same lidar system can measure both the nitrogen density and the water vapor by merely filtering the returned signal so that the detector measures the frequency characteristic of Raman scattering from one molecule or the other. Cooney[21] has compared the absolute humidity derived from Raman backscatter at heights up to 2 km with the humidity obtained from radiosonde measurements. The transmitter in his experiment was a high-power, frequency-doubled, Q-switched ruby laser which normally operated at 20-30 MW in 75 to 100 nsec pulses, and the receiver consisted of a high quality telescope. Cooney found a difference of approximately 13% in the value of the water vapor profile when integrated between .5 km and 2 km for the two measurements. Furthermore, the actual humidity profiles obtained by the radiosonde and the lidar were in good agreement. It is impossible, however, to rigorously determine the accuracy of the lidar system from these comparisons since the radiosonde measurements themselves were only accurate to ~ 10%.

The Raman signal must be extracted from the noise due to radiation from the background sky. During the day, this background radiation is approximately two orders of magnitude greater than the Raman signal from present systems. Consequently, all the Raman experiments described above were conducted at night to minimize the ambient flux. Cooney has proposed a technique for extending the use of Raman lidar to daytime[22]. The method requires that the Raman backscatter from two different atmospheric constituents, such as nitrogen and water vapor, be monitored simultaneously and the signals processed through a differential amplifier, thereby eliminating the high-intensity daylight flux common to both returns. With this technique, the relative concentrations of the two monitored constituents can be determined. Still, Raman measurements during daylight at ranges of interest to ballistic meteorology will require a significant improvement in the signal to noise ratio. As noted by Derr and Little, the Raman lidar will probably not reach its full potential as an atmospheric probe until powerful, efficient lasers are developed in the ultraviolet region below 290 nm, where the background solar flux is significantly reduced by ozone absorption in the stratosphere[23]. Alternatively, the signal can be increased

20. J.A. Cooney, "Remote Measurement of Atmospheric Water Vapor Profiles Using the Raman Component of Laser Backscatter", J. Appl. Met. 9, 182 (1970).
21. J.A. Cooney, "Comparisons of Water Vapor Profiles Obtained by Radiosonde and Laser Backscatter", J. Appl. Met. 10, 301 (1971).
22. J.A. Cooney, "A Method for Extending the Use of Raman LIDAR to Daytime", J. Appl. Met. 12, 888 (1973).
23. V.E. Derr and C.G. Little, "A Comparison of Remote Sensing of the Clear Atmosphere by Optical, Radio and Acoustic Radar Techniques", Appl. Opt. 9, 1976 (1970).

appreciably by the development of tunable lasers which exploit the resonance Raman effect. Meanwhile, increases in the power per laser pulse and pulse repetition frequency of existing laser systems will enhance the signal to noise ratio.

In addition to Raman scattering, the humidity has also been measured with a lidar operating in the resonance absorption mode. Taking advantage of the chance coincidence of a water vapor line at 694.38 nm with the emission line of the ruby laser, Schotland[24] was able to determine the water vapor profile to a height of 4 km from the ratio of the return at the resonance frequency to the return off resonance.

VI. LIDAR MEASUREMENTS OF TEMPERATURE

Once the density profile has been determined, for example from the Rayleigh component of the scattered radiation or by Raman scattering, the temperature profile can be calculated directly from the hydrostatic equation. Integration of the hydrostatic equation, Eq. (3.2), from ground where Z=0 and $p=p_o$ to an altitude h yields the following expression for the pressure at h:

$$p(h) = p_o - g \int_o^h \rho(Z)dZ \ . \tag{6.1}$$

After substituting for p(h) from the perfect gas law, Eq. (3.1), we can rewrite Eq. (6.1) as

$$T(h) = \frac{p_o - g\int_o^h \rho(Z)dZ}{R\,\rho(h)} \tag{6.2}$$

Therefore, the temperature profile can be determined from the density profile and a measurement of the pressure at ground level. However, this method requires that the density profile be accurate to within a few percent in order to yield reliable values for the temperature.

As mentioned in Sec. IV, the frequency of the radiation undergoing Rayleigh scattering is Doppler shifted by the thermal motion of the molecules, resulting in a gaussian spectrum whose width depends on the temperature. Fiocco and his colleagues took advantage of this property

24. R.M. Schotland, "Some Observations of the Vertical Profile of Water Vapor by a Laser Optical Radar", Proc. 4th Symp. on Remote Sensing of the Environ. (Univ. of Michigan, Ann Arbor, 1966) 273-283.

of the Rayleigh spectrum to measure the atmospheric temperature[25]. Using the Doppler broadened backscatter from an argon laser, they determined the temperature to an altitude of 4 km and found moderately good agreement with the results of a balloon sounding some distance away. Of all the lidar methods for measuring temperature, this technique comes closest to achieving the range required for ballistic meteorology with lasers that are currently available.

Cooney[26] has suggested another technique for measuring temperature based on the shape of the envelope of the Raman spectrum. For linear molecules, the rotational Raman spectrum consists of two branches positioned symmetrically along the frequency axis about the incident frequency. The Stokes branch consists of scattered radiation whose frequency is lower than that of the incident radiation and corresponds to an interaction in which the molecule is raised from an initial rotational level J to a level J + 2 within the same vibrational state. Conversely, the Anti-Stokes branch consists of lines which have a higher frequency than the incident radiation, corresponding to the transistion $J+2 \rightarrow J$. The intensity of a line in the Raman spectrum is proportional to the number density of molecules in the initial level of the corresponding interaction. For a gas in equilibrium, the density of molecules in a vibration-rotational state is related to the temperature through the Boltzmann factor, $\exp(-E/kT)$ where E is the quantum energy associated with the state. Therefore, the temperature can be extracted from the ratio of the intensities of two lines in the Raman spectrum. In a controlled experiment designed to demonstrate the feasibility of this technique, Salzman and Coney[27] were able to measure the atmospheric temperature at a range of 100 m with an accuracy ± 4°K. Of course, the Raman measurement of temperature suffers from the same difficulties as those discussed in the previous section with regard to Raman measurements of density.

Raman scattering is only one of the possible techniques for measuring the thermal distribution of rotational states. For example, Mason[28] has discussed an alternative scheme which probes the distribution of rotational states by measuring the resonance absorption at two lines within a rotational-vibrational band. However, this technique requires a laser tunable to the resonance frequencies of the two lines with a bandwidth less than the widths of the lines.

---

25. G. Fiocco, G. Benedetti-Michelangeli, K. Maischberger and E. Madonna, "Measurement of Temperature and Aerosol to Molecule Ratio in the Troposphere by Optical Radar", Nat. Phys. Sci. 229, 78 (1971).
26. J. Cooney, "Measurement of Atmospheric Temperature Profiles by Raman Backscattering", J. Appl. Met. 11, 108 (1972).
27. J.A. Salzman and T.A. Coney, "Atmospheric Temperature Measurements Using Raman LIDAR", NASA TN D-7679, 1974.
28. J.B. Mason, "LIDAR Measurement of Temperature: A New Approach", Appl. Opt. 14, 76 (1975).

VII. LIDAR MEASUREMENT OF WIND VELOCITY

Atmospheric aerosols play a dual role in lidar measurements. On the one hand, their presence hampers the measurement of density from the Rayleigh backscatter. At the same time, aerosols are effective tracers of the atmospheric wind, a point which is discussed in greater detail in the Appendix, and their motion can be monitored to yield wind velocities. Two approaches to the lidar measurement of wind velocity are currently under investigation. The first technique utilizes the Doppler shift of the Mie backscatter to determine the aerosol velocity, while in the second method the laser beam tracks scattering inhomogeneities as they are carried along by the mean wind. In this section, we will discuss both of these approaches in some detail.

When radiation of wavelength λ is incident on a particle moving with a nonrelativistic velocity $\vec{v}$, the angular frequency of the scattered radiation is shifted by an amount

$$\Delta\omega = \frac{4\pi |\vec{v}| \cos\theta}{\lambda} \tag{7.1}$$

where θ is the angle subtended by the particle velocity and the direction of scatter as shown below.

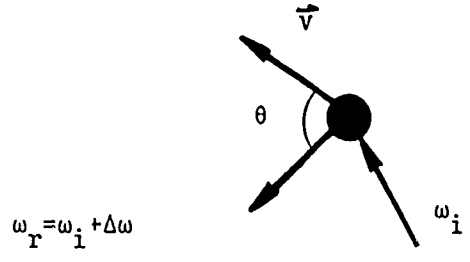

In the atmosphere, the velocities of the individual aerosols will be distributed about the local wind velocity due to Brownian motion, so that the intensity of the Mie backscatter will exhibit a frequency dependence. However, the Brownian velocity will generally be much less than the mean wind velocity, so that the return signal will have a sharp peak at

$$\omega_r = \omega_i + \frac{4\pi |\vec{u}| \cos\theta}{\lambda} \tag{7.2}$$

where ω_i and ω_r are the angular frequencies of the incident and reflected radiation, respectively, and $\vec{u}$ is the local wind velocity. According to Eq. (7.2), the shift in the frequency of the Mie backscatter, is a measure of the component of the wind in the direction of the scattered signal. Any device which determines flow velocity by exploiting this

Doppler shift with a laser providing the incident radiation is commonly referred to as a laser Doppler velocimeter (LDV). In atmospheric studies the frequency shift will be quite small. For example, the scattered radiation from a CO_2 laser (λ = 10.6 μ, $\omega = 1.8 \times 10^{14}$ rad/sec) will be only

$$\Delta\omega = 1.2 \times 10^{6} \, v \cos\theta \qquad (7.3)$$

where v is the particle velocity in m/sec and $\Delta\omega$ is in rad/sec.

For the monostatic lidar, corresponding to the case where the receiver and transmitter are colinear, the frequency shift will measure only the component of velocity along the line-of-sight of the transmitted beam. One method for obtaining the total vector velocity is to probe the region of uniform wind from three independent directions, but a more accurate system employs a conical scan of the atmosphere at a fixed altitude, analagous to the configuration commonly used in radar measurements [29].

The feasibility of using a focused laser Doppler velocimeter to measure wind velocity was demonstrated experimentally in 1972 by Lawrence, et al.[14,30] who probed the atmosphere to an altitude of 450m with a 25w CO_2 laser. The Doppler shift of the scattered radiation was determined by a heterodyne technique, in which the return signal is mixed with a portion of the original laser beam to produce a signal modulated at the frequency of the Doppler shift. Jeffreys and Bilbro[31] later incorporated the technique into a conically scanning system designed to measure aircraft wake vortices and wind profiles. Their velocimeter is capable of measuring velocities up to 60 m/sec with a resolution of .6 m/sec at ranges up to 600m.

For longer ranges, a system based on an unfocused, pulsed laser is required to provide adequate range resolution. Benedetti-Michelangeli and his associates were the first to use a pulsed laser Doppler technique to measure atmospheric winds[32]. The pulse train in their experiments

29. T.R. Lawrence, M.C. Krause, C.E. Craven, L.K. Morrison, J.A. L. Thomson, W.C. Cliff and R.M. Huffaker, "A Laser Doppler System for the Remote Sensing of Boundary Layer Winds in Clear Air Conditions", Preprint Vol. 16th Radar Meteorology Conf, 320 (1975).
30. T.R. Lawrence, M.C. Krause, L.K. Morrison, and C.E. Craven, "A Study on Laser Doppler Velocimeter Atmospheric Wind Interrogation Systems", LMSC-HREC TRD 306888, 1973.
31. H.B. Jeffreys and J.W. Bilbro, "Development of a Laser Doppler System for the Detection and Monitoring of Atmospheric Disturbances", NASA TMX-64981, 1975.
32. G.Benedetti-Michelangeli, F. Congeduti and G. Fiocco, "Measurement of Aerosol Motion and Wind Velocity in the Lower Troposphere by Doppler Optical Radar", J. Atmos. Sci. 29, 906 (1972).

was generated by modulating a .2w continuous argon laser and consisted of 10 μsec pulses separated by 65μsec. In this case, the Doppler shift was measured directly with an interferometer. Their experiments were conducted at night to limit the radiation from the background sky, and they could probe only to an altitude of 750m. The authors estimated the rms error of the velocity measurement to be ± .27 m/sec, and noted that the range and accuracy could be increased substantially with an optimized system.

Although the feasibility of laser Doppler measurements of wind velocity has been demonstrated, further research is required before the technique can be used to determine ballistic winds. The experiments to date have been limited to ranges less than a kilometer, far short of the tens of kilometers required, and neither the heterodyne detector nor the interferometric technique is presently capable of measuring the Doppler shift of radiation scattered at high altitudes. The interferometric technique requires detection of a weak return signal against the radiation of the background sky. The return signal can be enhanced, of course, by the development of more powerful laser sources. The heterodyne process is limited by the constraint that the backscattered radiation be nearly spatially coherent with the original laser radiation at the photodetector[33]. Atmospheric turbulence severely distorts the phase surfaces of the transmitted and scattered radiation, so that the spatial coherence degrades with range. Systems are being studied, however, whereby beams with essentially the same atmospheric-induced distortion are combined so that spatial coherence is maintained[33].

The second method for determining winds by lidar relies on the spatial inhomogeneity of the density of atmospheric aerosols. These inhomogeneities can result from turbulence and humidity variations in the atmosphere, or from intermittent aerosol sources. Lidar data shows that large inhomogeneities (on the order of 100m in width) are effective velocity tracers, moving consistently with the mean wind. Since the laser backscatter is strongly dependent on aerosol density, it is possible to recognize and track these density variations with lidar. By cross-correlating the scattered radiation from a pulsed, ruby laser as a function of time lag, Eloranta, et al.[34] were able to monitor the motion of large-scale inhomogeneities and thereby deduce wind velocities. The laser in their experiment was pointed in the direction of the surface wind and inclined at a 10° elevation angle.

33. J.A. Reagan and R.M. Schotland, "The Use of LIDAR in Atmospheric Measurements", 3rd Symp. on Meteorological Observations and Instrumentation, Preprint Volume, 157 (1976).
34. E.W. Eloranta, J.M. King and J.A. Weinman, "The Determination of Wind Speeds in the Boundary Layer by Monostatic LIDAR", J. Appl. Met. 14, 1485 (1975).

In a typical observation period, 50-200 backscatter profiles were recorded at approximately 20 second time intervals and correlated. In this manner, the line-of-sight component of the wind was obtained for altitudes up to 1.3 km, corresponding to a slant range of 7.5 km. The wind component derived from their soundings was compared with the wind profile derived from concurrent pilot balloon measurements and found to be consistent.

The reliability of the time-lag technique depends on how well the scattering profiles at successive times can be correlated. In practice, a number of factors will limit the correlation. The backscatter signal from the aerosol "clouds" will be degraded by noise due to non-persistent small eddies and gross features which do not convect with the wind. Furthermore, the aerosol structure between shots may change as a result of turbulent mixing, thereby altering the backscatter from the cloud. Finally, in the experiment of Eloranta where the laser is pointed in a fixed direction, the inhomogeneity may be swept out of the path of the lidar beam by the cross beam component of the wind. (This deficiency can be corrected, however, by directing the beam vertically and scanning conically at increasing radii and with sufficient frequency that the inhomogeneity does not cross the cone unilluminated[23]. This technique has the additional advantage of not requiring an a priori assumption of the wind direction.) In their studies, Eloranta et al. found that the maximum value of the cross correlation occurred at altitudes between 500 and 900 m. The correlation decreases at lower altitudes because aerosol inhomogeneities tend to be smaller and less persistent near the surface. At higher altitudes, where the lidar returns are weak, the correlation is degraded by statistical shot noise. Consequently, probing at high altitudes may require introduction of artificial aerosols to enhance the inhomogeneity and increase the strength of the signal. The necessity of introducing artificial tracers would, however, eliminate one of the major advantages of laser probing over the rawinsonde system.

It is noteworthy that the lidar methods for measuring velocity do not require the laser radar equation to interpret the returns since the velocity information is not contained in the intensity of the backscattered signal. Rather, the velocity is derived from the shift in frequency of the Mie backscatter in the LDV method, and from the correlation in the backscatter associated with the movement of an inhomogeneity in the transit scheme.

VIII. CONCLUSIONS

Prompt, reliable monitoring of the atmosphere near the artillery site is necessary in order to correct the aim for the effects of atmospheric forces on the shell trajectory. The rawinsonde system currently used to obtain these measurements is limited by several factors, the most serious being the length of time required for

completing a sounding. Lidar is one technique that can significantly improve the timeliness of meteorological measurements. Experiments have demonstrated that laser probing is capable of determining all the relevant parameters, although a lidar system that simultaneously monitors the density, temperature, humidity and wind velocity has not yet been developed. The experiments have generally been limited to altitudes of a few kilometers, and in some cases, particularly the Raman measurements, only nighttime operation was possible. However, future developments in laser technology and detection techniques could ease these constraints. Meanwhile, a ballistic meteorology system could be developed which would use lidar for low-altitude, continuous monitoring of one or more atmospheric parameters, complemented by conventional measurements where necessary.

REFERENCES

1. Department of the Army Field Manual FM 6-15, Artillery Meteorology (1970).

2. U.S. Standard Atmosphere, 1962 (US Government Printing Office, Washington, 1962), Ch 1.

3. E.R. Reiter, "Fundamental Problems of Atmospheric Science", in Remote Sensing of the Troposphere, edited by V.E. Derr (US Government Printing Office, Washington, 1972).

4. O.P. Bruno, "Effects of Ballistic and Meteorological Variables On Accuracy of Artillery Fire", BRL Memorandum Report 1210, US Army Ballistic Research Laboratories, 1959. (AD #219226)

5. R. Bellucci, "Analysis of Ballistic Meteorological Effects on Artillery Fire", USASRDL Technical Report 2224, 1961.

6. K.M. Barnett, E.A. Blomerth and H.H. Monahan, "Plan for the Atmospheric Sciences Laboratory Artillery Meteorological Comparisons", US Army ECOM, 1974.

7. J.H. Shinn and H.W. Maynard, "On the Sensitivity of Selected Typical Army Operations to Weather Effects", US Army ECOM-5547, 1974.

8. G. Fiocco and L.D. Smullin, "Detection of Scattering Layers in the Upper Atmosphere (60-140 km) by Optical Radar", Nature 199, 1275 (1963).

9. O.K. Kostko, "Use of Laser Radar in Atmospheric Investigations (Review)", Sov. J. Quant. Electron. 5, 1161 (1976).

10. C.P. Wang, "Application of Lasers in Atmospheric Probing", Acta Astron. 1, 105 (1974).

11. R.T.H. Collis, "LIDAR", Appl. Opt. 9, 1782 (1970).

12. R.G. Strauch and A. Cohen, "Atmospheric Remote Sensing With Laser Radar", in Remote Sensing of the Troposphere edited by V.E. Derr (US Government Printing Office, Washington, 1972).

13. F.S. Harris, "Laser Applications to Atmospheric Sciences-A Bibliography", NASA CR-2536. 1975.

14. T.R. Lawrence, D.J. Wilson, C.E. Craven, L.P. Jones, R.M. Huffaker and J.A.L. Thomson, "A Laser Velocimeter for Remote Wind Sensing", Rev. Sci. Inst. 43, 512 (1972).

15. D. Leonard, "Observation of Raman Scattering from the Atmosphere Using a Pulsed Nitrogen Ultraviolet Laser", Nature 216, 142 (1967).

16. J.A. Cooney, "Measurements on the Raman Component of Laser Atmospheric Backscatter", Appl. Phys. Lett. 12, 40 (1968)

17. S.H. Melfi, J.D. Lawrence, and M.P. McCormick, "Observation of Raman Scattering by Water Vapor in the Atmosphere", Appl. Phys. Lett. 15, 295 (1969).

18. S.H. Melfi, "Remote Measurements of the Atmosphere Using Raman Scattering", Appl. Optics 11, 1605 (1972).

19. M.J. Garvey and G.S. Kent, "Raman Backscatter of Laser Radiation from the Stratosphere", Nature 248, 124 (1974).

20. J.A. Cooney, "Remote Measurement of Atmospheric Water Vapor Profiles Using the Raman Component of Laser Backscatter", J. Appl. Met. 9, 182 (1970).

21. J.A. Cooney, "Comparisons of Water Vapor Profiles Obtained by Radiosonde and Laser Backscatter", J. Appl. Met. 10, 301 (1971).

22. J.A. Cooney, "A Method for Extending the Use of Raman LIDAR to Daytime", J. Appl. Met. 12, 888 (1973).

23. V.E. Derr and C.G. Little, "A Comparison of Remote Sensing of the Clear Atmosphere by Optical, Radio and Acoustic Radar Techniques", Appl. Opt. 9, 1976 (1970).

24. R.M. Schotland, "Some Observations of the Vertical Profile of Water Vapor by a Laser Optical Radar", Proc. 4th Symp. on Remote Sensing of the Environ. (Univ. of Michigan, Ann Arbor, 1966) 273-283.

25. G. Fiocco, G. Benedetti-Michelangeli, K. Maischberger and E. Madonna, "Measurement of Temperature and Aerosol to Molecule Ratio in the Troposphere by Optical Radar", Nat. Phys. Sci. 229, 78 (1971).

26. J. Cooney, "Measurement of Atmospheric Temperature Profiles by Raman Backscattering", J. Appl. Met. 11, 108 (1972).

27. J.A. Salzman and T.A. Coney, "Atmospheric Temperature Measurements Using Raman LIDAR", NASA TN D-7679, 1974.

28. J.B. Mason, "LIDAR Measurement of Temperature: A New Approach", Appl. Opt. 14, 76 (1975).

29. T.R. Lawrence, M.C. Krause, C.E. Craven, L.K. Morrison, J.A.L. Thomson, W.C. Cliff and R.M. Huffaker, "A Laser Doppler System for the Remote Sensing of Boundary Layer Winds in Clear Air Conditions", Preprint Vol. 16th Radar Meteorology Conf, 320 (1975).

30. T.R. Lawrence, M.C. Krause, L.K. Morrison, and C.E. Craven, "A Study on Laser Doppler Velocimeter Atmospheric Wind Interrogation Systems", LMSC-HREC TRD 306888, 1973.

31. H.B. Jeffreys and J.W. Bilbro, "Development of a Laser Doppler System for the Detection and Monitoring of Atmospheric Disturbances", NASA TMX-64981, 1975.

32. G. Benedetti-Michelangeli, F. Congeduti and G. Fiocco, "Measurement of Aerosol Motion and Wind Velocity in the Lower Troposphere by Doppler Optical Radar", J. Atmos. Sci. 29, 906 (1972).

33. J.A. Reagan and R.M. Schotland, "The Use of LIDAR in Atmospheric Measurements", 3rd Symp. on Meteorological Observations and Instrumentation, Preprint Volume, 157 (1976).

34. E.W. Eloranta, J.M. King and J.A. Weinman, "The Determination of Wind Speeds in the Boundary Layer by Monostatic LIDAR", J. Appl. Met. 14, 1485 (1975).

APPENDIX

RESPONSE OF AEROSOL PARTICLES TO THE MEAN WIND

In this appendix the response of a small, aerosol particle to variations in the wind velocity will be examined. For definiteness, the particle is taken to be spherical although aerosols can actually take on a wide variety of shapes. The momentum equation for a particle in a coordinate frame fixed to the earth with the z-axis in the vertical direction is[A.1]

$$m \frac{d\bar{u}}{dt} = \bar{F}_D + m_a \frac{d}{dt} (\bar{v} - \bar{u}) + (m_o - m) g \hat{z} \qquad (A.1)$$

where m is the mass of the particle; m_a is its apparent mass and $\bar{u}$ is its velocity; $\bar{F}_D$ is the drag force on the particle; $\bar{v}$ is the wind velocity; m_o is the mass of air displaced by the particle and g is the acceleration due to gravity. The time derivative is the total derivative given by

$$\frac{d}{dt} = \frac{\partial}{\partial t} + \bar{u} \cdot \bar{\nabla} \quad .$$

The second term on the right hand side of Eq. (A.1) results from the momentum interchange between the particle and the flow field. For a sphere the apparent mass is given by

$$m_a = \tfrac{1}{2} m_o \quad . \qquad (A.2)$$

The last term on the right hand side of Eq. (A.1) is the net buoyant force on the sphere.

The general expression for the drag force is

$$\bar{F}_D = \tfrac{1}{2} \rho C_D A |\bar{v} - \bar{u}| (\bar{v} - \bar{u}) \qquad (A.3)$$

where ρ is the fluid density, C_D is the drag coefficient of the particle and A is its cross-sectional area. The drag coefficient, in turn, is a function of the Reynolds number,

$$Re = \frac{2r|\bar{v} - \bar{u}|\rho}{\mu} \qquad (A.4)$$

where r is the particle radius and μ is the viscosity of air.

Equations (A.1) - (A.3) apply to any rigid, spherical mass, regardless of size, as long as the hydrodynamic description is valid. For an aerosol particle, this restriction requires that the particle

A.1 G.H. Fichtl, "The Response of Balloon and Falling Sphere Wind Sensors in Turbulent Flows", NASA TN D-7049, 1971.

radius be much larger than the mean free path of air molecules ($\sim 10^{-7}$ m at STP). Equation (A.1) cannot, in general, be solved analytically due to the nonlinear drag term. However, in the Stokes flow regime ($Re \leq 1$) the drag coefficient is approximately

$$C_D = \frac{24}{Re} \tag{A.5}$$

and the drag force has the simple form

$$\bar{F}_D = 6\pi r\mu(\bar{v}-\bar{u}) \ . \tag{A.6}$$

Fortunately, Stokes flow is applicable to many cases of aerosol motion.

In order to determine how rapidly the particle velocity can adjust to a change in the external flow field, we consider the following model problem. We assume that for time $t < 0$ the particle is in equilibrium with the flow field so that

$$\bar{u} = \bar{v}_o + w\,\hat{z} \tag{A.7}$$

where $\bar{v}_o$ is the local flow velocity at the particle's location and

$$w = \frac{g(m_o-m)}{6\pi\mu r} \tag{A.8}$$

is the particle's terminal velocity (the velocity at which the drag force in the vertical direction equals the net buoyant force). At time t=0, the flow velocity is changed instantaneously to a velocity $\bar{v}_1$ and then remains constant in time. Furthermore, it is anticipated that the particle response will be sufficiently rapid that $\bar{v}_1$ can also be considered spatially invariant during the time interval of interest. Finally, the velocity differential $|\bar{v}_1-\bar{u}|$ is assumed small enough for the Stokes flow approximation to be valid. For these conditions Eq. (A.1) becomes

$$(m_a + m)\frac{d}{dt}(\bar{u}-\bar{v}_1) = -6\pi r\mu(\bar{u}-\bar{v}_1) + (m_o-m)g\hat{z} \ . \tag{A.9}$$

The solution to Eq. (A.9) subject to the initial condition given by Eq. (A.7) is

$$\bar{u} = \bar{v}_1 + w\,\hat{z} + (\bar{v}_o - \bar{v}_1)e^{-t/\tau} \tag{A.10}$$

where

$$\tau = \frac{m_a + m}{6\pi\mu r} \ . \tag{A.11}$$

According to Eq. (A.10) the particle re-establishes its equilibrium with the external flow field exponentially with a characteristic time τ given by Eq. (A.11). Furthermore, the particle velocity asymptotically approaches the sum of the environmental flow velocity and the particle's terminal velocity.

Expressing the response time and the terminal velocity in terms of the density of the aerosol particle, ρ_a, and the ambient air density, ρ, we obtain

$$\tau = \frac{2\rho_a r^2}{9\mu} \left(1 + \tfrac{1}{2} \frac{\rho}{\rho_a}\right) \tag{A.12}$$

and

$$w = - g\tau \frac{\rho_a - \rho}{\rho_a + \frac{1}{2}\rho} \quad . \tag{A.13}$$

For solid and liquid aerosol particles, the ratio $\rho/\rho_a \ll 1$ so that

$$\tau = \frac{2\rho_a r^2}{9\mu} \tag{A.14}$$

and

$$w = - g\tau. \tag{A.15}$$

For example, a solid aerosol particle with a radius of 5×10^{-6}m and a density of 1 gm/cm^3 in atmospheric pressure air ($\mu = 1.73 \times 10^{-4}$ gm/cm sec), has a response time $\tau = 3 \times 10^{-4}$ sec and a terminal velocity w = .30 cm/sec. This extremely short relaxation time makes aerosols ideal tracers of atmospheric motion.

Equation (A.1) with the general drag term has also been used to study the response of large balloon sensors. Reed[A.2], Eckstrom[A.3], and Fichtl[A.4] have analyzed the balloon's response to a steady, horizontal wind field varying linearly with height. They derived a balloon response time

$$\tau = \frac{m_a + m}{|m_o - m|} \frac{w}{g} \tag{A.16}$$

A.2 W.H. Reed, "Dynamic Response of Rising and Falling Balloon Wind Sensors With Application to Estimates of Wind Loads on Launch Vehicles", NASA TN D-1821, 1963.

A-3 G.T. Schjeldahl Co., "Theoretical Study and Engineering Development of Jimsphere Wind Sensor", Final Report, Contract NAS 8-11158, 1965.

A.4 G.H. Fichtl, "Behavior of Spherical Balloons in Wind Shear Layers", J. Geophys. Res. 77, 3931 (1972).

where the quantities have the same meaning as in the previous analysis except that they now refer to properties of the balloon. The balloon's terminal velocity is given by the implicit relation

$$\tfrac{1}{2} \rho A C_D w^2 = g (m_o - m) \qquad (A.17)$$

where C_D is the drag coefficient for the balloon and A is its cross sectional area. (In fact, the aerosol particle response time can be expressed in the same form as Eq. (A.16) by expressing τ in Eq. (A.11) in terms of the particle's terminal velocity given by Eq. (A.8).) For typical rising and falling balloon spheres, τ is on the order of a second and w is a few meters per second[A.2]. Therefore, aerosol tracers are far more sensitive to wind variations than typical meteorological balloons. Although the sensitivity is not critical for determining horizontal winds averaged over several hundred meters, it would be important for measurements of the vertical component of the wind.

At present the ballistic trajectory is not corrected for vertical wind effects since balloon sensors are not capable of providing an accurate determination of the vertical wind. The balloon motion due to vortex separation and the spatially varying buoyant and drag forces obscures the effect of the vertical wind on the balloon's trajectory[A.5]. On the other hand, the terminal velocity of aerosols is so low that the particle achieves equilibrium with the wind velocity before variations in density become appreciable. Also, since the terminal velocity is only on the order of a centimeter per second, the aerosol's vertical velocity would be an accurate reflection of the vertical wind velocity. It should be mentioned, however, that in the atmospheric boundary layer the vertical wind velocity is generally much smaller than the horizontal wind velocity so that its influence on the ballistic trajectory may not be significant.

A.5 R.E. DeMandel and S.J. Krivo, "Radar/Balloon Measurement of Vertical Air Motions Between the Surface and 15 km", J. Appl. Met. 10, 313 (1971).

APPENDIX REFERENCES

A.1 G.H. Fichtl, "The Response of Balloon and Falling Sphere Wind Sensors in Turbulent Flows", NASA TN D-7049, 1971.

A-2 W.H. Reed, "Dynamic Response of Rising and Falling Balloon Wind Sensors With Application to Estimates of Wind Loads on Launch Vehicles", NASA TN D-1821, 1963.

A-3 G.T. Schjeldahl Co., "Theoretical Study and Engineering Development of Jimsphere Wind Sensor", Final Report, Contract NAS 8-11158, 1965.

A-4 G.H. Fichtl, "Behavior of Spherical Balloons in Wind Shear Layers", J. Geophys. Res. 77, 3931 (1972).

A-5 R.E. DeMandel and S.J. Krivo, "Radar/Balloon Measurement of Vertical Air Motions Between the Surface and 15 km", J. Appl. Met. 10, 313 (1971).

DISTRIBUTION LIST

No. of Copies	Organization
12	Commander Defense Documentation Center ATTN: DDC-TCA Cameron Station Alexandria, VA 22314
1	Commander US Army Materiel Development and Readiness Command ATTN: DRCDMA-ST 5001 Eisenhower Avenue Alexandria, VA 22333
1	Commander US Army Aviation Research and Development Command ATTN: DRSAV-E 12th and Spruce Streets St. Louis, MO 63166
1	Director US Army Air Mobility Research and Development Laboratory Ames Research Center Moffett Field, CA 94035
1	Commander US Army Electronics Command ATTN: DRSEL-RD Fort Monmouth, NJ 07703
1	Commander US Army Missile Research and Development Command ATTN: DRDMI-R Redstone Arsenal, AL 35809
1	Commander US Army Tank Automotive Development Command ATTN: DRDTA-RWL Warren, MI 48092
2	Commander US Army Mobility Equipment Research & Development Cmd ATTN: Tech Docu Cen, Bldg. 315 DRSME-RZT Fort Belvoir, VA 22060
1	Commander US Army Armament Materiel Readiness Command Rock Island, IL 61202
1	Commander US Army Harry Diamond Labs ATTN: DRXDO-TI 2800 Powder Mill Road Adelphi, MD 20783
1	Director US Army TRADOC Systems Analysis Activity ATTN: ATAA-SA White Sands Missile Range NM 88002
1	Director National Aeronautics and Space Administration Langley Research Center ATTN: Dr. E. V. Browell MS 401A Hampton, VA 23665
1	Director National Aeronautics and Space Administration Marshall Space Flight Center ATTN: Mr. R. M. Huffaker Optics and RF Systems Division Huntsville, AL 35812

PRECEDING PAGE BLANK

DISTRIBUTION LIST

No. of Copies	Organization
1	Science Applications, Inc. ATTN: Mr. S. Howie 2028 Powers Ferry Rd Suite 260 Atlanta, GA 30339
3	University of Florida Dept of Engineering Sciences ATTN: Prof. K. T. Millsaps Prof. D. R. Keefer Prof. B. M. Leadon Gainesville, FL 32603
	Aberdeen Proving Ground
	Marine Corps Ln Ofc Dir, USAMSAA